Bulk defects and surface state dynamics in topological insulators: The effects of electron beam irradiation on the ultrafast relaxation of Dirac fermions in Bi 2 Te 3

L. Khalil, E. Papalazarou, M. Caputo, N. Nilforoushan, L. Perfetti, A. Taleb-Ibrahimi, M. Konczykowski, A. Hruban, A. Wołoś, L. Krusin-Elbaum, et al.

Bulk defects and surface state dynamics in topological insulators: the effects of electron beam irradiation on the ultrafast relaxation of Dirac fermions in Bi_2Te_3

L. Khalil,[1,2] E. Papalazarou,[1] M. Caputo,[1] N. Nilforoushan,[1] L. Perfetti,[3] A. Taleb-Ibrahimi,[4] M. Konczykowski,[3] A. Hruban,[5] A. Wołoś,[6] L. Krusin-Elbaum,[7] and M. Marsi[1]

[1] *Laboratoire de Physique des Solides, CNRS, Univ. Paris-Sud, Université Paris-Saclay, 91405 Orsay Cedex, France*
[2] *Synchrotron SOLEIL, Saint Aubin BP 48, Gif-sur-Yvette F-91192, France*
[3] *Laboratoire des Solides Irradiés, Ecole Polytechnique, CNRS, CEA, Université Paris-Saclay, 91128 Palaiseau cedex, France*
[4] *UR1-CNRS/Synchrotron SOLEIL, Saint Aubin BP 48, Gif-sur-Yvette F-91192, France*
[5] *Institute of Electronic Materials Technology, 01-919 Warsaw, Poland*
[6] *Faculty of Physics, University of Warsaw, 02-093 Warsaw, Poland*
[7] *Department of Physics, The City College of New York, CUNY, New York, NY 10031, USA*

(Dated: April 20, 2018)

One of the most important challenges in the study of topological insulators is the realization of materials that are really insulating in the bulk, in order to emphasize quantum transport in the protected surface states. Irradiation with electron beams is a very promising approach towards this goal. By studying a series of samples of the prototype 3D topological insulator Bi_2Te_3 we show that, while the topological properties of Dirac surface states are preserved after electron irradiation, their ultrafast relaxation dynamics is very sensitive to the related modifications of the bulk properties. Using time- and angle-resolved photoelectron spectroscopy, we can reveal two distinct relaxation regimes after optical excitation for non-irradiated and high-energy electron beam irradiated samples. While the faster regime, corresponding to the first few picoseconds, presents a similar temporal evolution of the photoexcited population for all studied samples, the slower regime is strongly influenced by the controlled generation of defects in the bulk lattice. By adjusting the irradiation parameters in this class of materials, one can thus not only change the bulk transport properties, but also tune the ultrafast response of the topological surface states.

PACS numbers: 78.47.J-,79.60.-i,73.20.-r

I. INTRODUCTION

During the last years, three-dimensional topological insulators (3D TIs) have attracted a lot of interest due to their unconventional and unique properties [1–6]. While they are narrow-band semiconductors in the bulk, these materials possess gapless and topologically protected two-dimensional surface states (2D SSs), characterized by a Dirac-type linear energy-momentum electronic dispersion. Thanks to the combined action of spin-orbit coupling and of time-reversal symmetry, the relativistic fermions travelling in the spin-momentum locked SSs are insensitive to back-scattering in the presence of non-magnetic defects and impurities [7–9]. Distressingly, prototype narrow-gap TIs, such as Bi_2Te_3 and Bi_2Se_3 [10], commonly present lattice defects, i.e. vacancies and anti-sites, generated during crystal growth [11]. Consequently, the conduction through the surface channels is unavoidably intermixed with detrimental bulk conductivity [12, 13]; this hinders the access to a genuine surface electronic transport indispensable for promising technological applications, such as spintronics [14] or topological quantum computing [3].

Several attempts to decrease the significant bulk carrier contribution were based on chemical doping [15, 16], increasing the surface-to-bulk ratio using nanostructuring which can be performed through mechanical exfoliation or growth of TI nanowires and nanoribbons [17, 18], epitaxial growth of TI/II-VI semiconductor superlattices [19, 20], and irradiation by high-energy electron beams: in particular, intrinsic quantum transport measurements and angle-resolved photoemission spectroscopy (ARPES) revealed that a technique based on irradiation with swift ($\sim$ 2.5 MeV energy) electron beams at specific electron doses [21] doesn't affect the Dirac energy dispersion—immmune to disorder—and offers a path to large scale transport in topological SSs. Furthermore, this experimental study has indicated that it is possible, by following a thermal protocol, to tune the band position from the irradiation-induced *n*-type back towards the charge neutrality point where the system remains for months. At the microscopic level, this is related to the creation of vacancy-interstitial pairs (Frenkel defects) in the bulk material: consequently, these results call for more extensive investigations to unveil if and how the irradiation procedure affects the properties of the surface Dirac fermions.

In this paper, we present a time-resolved ARPES (trARPES) study of Bi_2Te_3 compounds under various irradiation conditions. Thanks to the combination of time, momentum and energy resolution [22, 23], our results reveal the impact of the swift electron irradiation on the

scattering and carrier relaxation dynamics in response to ultrafast optical excitation. In particular, we demonstrate that the induced disorder affects the ultrafast relaxation times of the out-of-equilibrium transient carrier population.

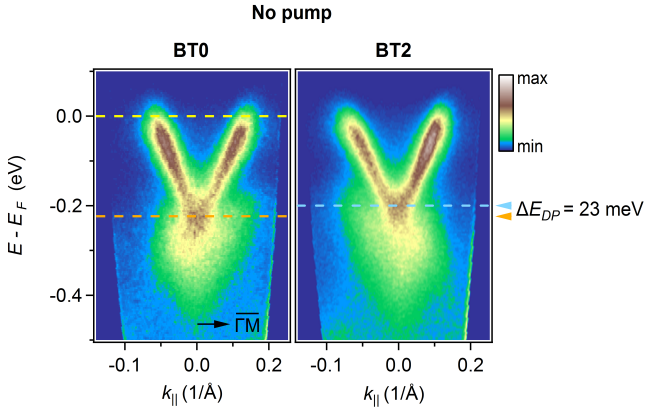

FIG. 1: (color online). Comparison of the photoelectrons intensity maps along the $\overline{\Gamma M}$ direction for the non-irradiated BT0 and the irradiated BT2 crystals. The detected DP positions differ from a binding energy of 23 meV between the two ARPES images.

II. METHOD AND EXPERIMENTAL DETAILS

We investigate high-quality Bi_2Te_3 single crystals grown with a modified Bridgman method. Two of these crystals, namely BT1 and BT2, have been irradiated with a swift electron dose of 1 C/cm^2 and 1.7 C/cm^2, respectively. All studied crystals come from the same boule. Carrier density was calculated from *ex situ* transport and Shubnikov–de Haas oscillations measurements, and was evaluated to be 4×10^{18} cm^{-3} for the *p*-doped non-irradiated sample, designated as BT0. Directly after an irradiation dose of 1 C/cm^2 and 1.7 C/cm^2, the conduction becomes *n*-type and the carrier concentration is 1.7 $\times$ 10^{19} cm^{-3} and 1.97 $\times$ 10^{19} cm^{-3}, at 105 K, respectively.

All samples were precisely oriented along the $\overline{\Gamma M}$ high symmetry direction and cleaved *in situ* with a top-post at room temperature under ultrahigh vacuum conditions (base pressure better than 2.5×10^{-10} mbar). After cooling down the samples, all trARPES measurements were carried out at a base temperature of 130 K using the FemtoARPES setup. A commercial Ti-Sapphire laser generates 35 fs pulses centered at 1.58 eV photons energy with a repetition rate of 250 KHz. The fourth harmonic of 6.32 eV is generated by cascade frequency mixing in BBO non-linear crystals (β-BaB_2O_4) from the 1.58 eV initial output laser power that is used to pump the transient populated band structure. Both 1.58 eV pump and 6.32 eV probe beams were focused almost collinearly at an angle of 45° with respect to the surface normal. The pump-probe photoemission measurements can be performed with an overall temporal resolution of 80 fs and an energy resolution of 60 meV. (A full description of our experimental setup and of its specifics can be found in [24, 25].) The use of a 6.32 eV probe gives access to a narrow portion of *k*-space, but sufficient in this case to observe the unoccupied SSs at the $\bar{\Gamma}$ point. The out-of-equilibrium spectra were recorded using linear *S*-polarized 6.32 eV photons and were collected under an infrared pump fluence of 0.15 mJ/cm^2.

III. RESULTS AND DISCUSSION

In Fig. 1, we compare conventional ARPES yields of a non-irradiated and an irradiated sample. It should be noted that the BT2 sample, after irradiation with 1.7 C/cm^2 of terminal electron dose, was kept at room temperature for more than one month. The aim of this was to allow vacancies to diffuse in order to determine whether the irradiated compound would regain its initial properties. At first sight, we clearly remark that the binding energies of the Dirac point (DP) with respect to the surface chemical potential E_F, indicated by a yellow dashed line, are different for the two samples. Quantitatively, the DPs, delimited by orange and blue dashed lines, present a shift of 23 meV between the BT0 and the BT2 specimens. The positions were found by fitting the energy distribution curves near $\bar{\Gamma}$ with a Gaussian function. This reflects that the irradiated sample does not retrieve its original state of equilibrium after defect migration despite the preservation of the electronic Dirac cone spectrum against irradiation.

To better understand the consequences of the electron beam irradiation on the sample response to ultrafast light pulses, we have performed a series of trARPES measurements. For this technique, pump photons excite hot electrons into the empty states, giving access to the band structure and the ultrafast time evolution of the transient electron population. As a representative example, we present in Fig. 2(a), images obtained for selected time delays on the freshly irradiated BT1 sample, i.e., the trARPES study was conducted immediately after the swift electron irradiation. Similar results were obtained also for the other samples, whose time evolutions are presented in Fig. 2(b).

Before the arrival of the infrared pump beam, at negative delays—equivalent to a time scale of 4 μs, i.e., to a complete relaxation of the system—we probe the electronic structure in its ground state: by comparing the photoemission signal at negative delays with the one obtained with no pump (see the upper-left corner of Fig. 2(a)), we verified that residual out-of-equilibrium effects such as surface photovoltage [26] were negligibly small. Thus, the photoelectron intensity spectrum taken

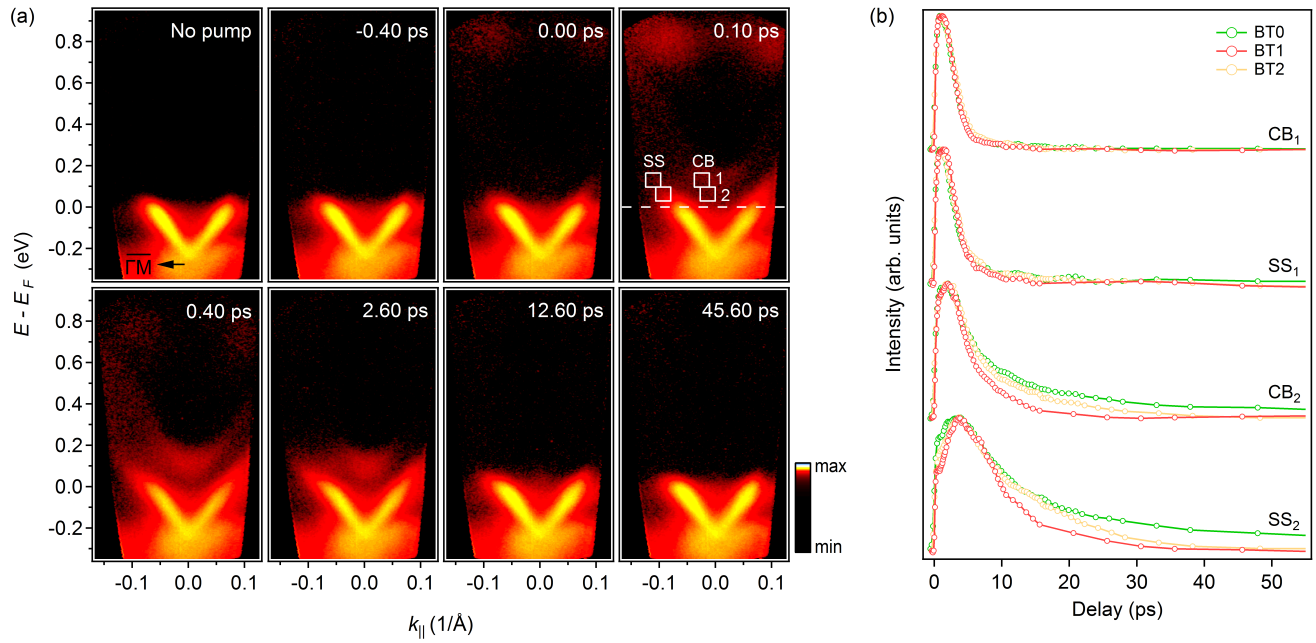

FIG. 2: (color online). Out-of-equilibrium dynamics of the photoexited electronic states. (a) trARPES sequence near the $\bar{\Gamma}$ point for various pump-probe delays for the freshly irradiated specimen. White dashed line indicates the E_F. The color intensity is displayed in logarithmic scale to make the signal from the unoccupied electronic band structure more discernible. (b) Transient photoemission intensity within the integration windows 1 and 2 (presented at Δt = 10 ps time delay in (a)) for the three sibling Bi_2Te_3 samples.

at -0.40 ps time delay [Fig. 2(a)] shows electronic band structure at equilibrium, right before any excitation effect. Following the pump photoexcitation at $\Delta t = 0$ ps, a transient excited electron population is oberved at energies ∼0.6—0.8 eV above E_F. Note that the SSs and the lower-lying conduction band (CB) are not directly populated (as it was already discussed by [27]). These highly excited electronic states dissipate rapidly, triggering a cascade of intraband and interband transitions through recombination procedures acting as a source of electrons for the low-lying CB and SSs. In order to obtain a quantitative picture on the characteristic relaxation times of the involved transient electronic population, we integrated over different k-E integration windows delineated as 1 and 2. As discussed in previous works [28, 29], the dynamics depend on the precise choice of the energy-momentum window: for the sake of comparison, the SS_2 and CB_2 boxes were taken at 28 meV above E_F for all our Bi_2Te_3 samples and Fig. 2(b) depicts the respective transient electronic populations.

Quantitatively, the relaxation times of SS_1 and CB_1 are summarized in Table I. The characteristic lifetime of the excess electron population for the 1–2 k-E SS and CB regions were extracted by fitting our data with a single or a double decay exponential function. For each sample, the SS_1 and the CB_1 possess similar scattering times indicating that SS_1 and CB_1 present a parallel evolution and an effective carrier exchange takes place between the two bands (interband scattering). Evidently, for the ultrafast dynamics (during the first few picoseconds), this characteristic times τ_1 are mostly due to the electron-phonon coupling for both surface and bulk bands. However, BT0 exhibit a second Dirac fermion lifetime τ_2, having a value of 29.74 ps, reflecting the presence of an additional filling channel, probably a diffusion channel [23]. Besides, we notice that the irradiation process does not affect the order of magnitude of the electron decay times of SS_1 and CB_1, the values are in the same range and almost similar, i.e., around 2 ps for SS_1 and for CB_1 for the three crystals, but suppress the long Dirac electron lifetime of the SSs by creating additional recombination channels by means of defects induced by the irradiation procedure. Moreover, the long lasting excited SS_1 population persists for more than 10 ps; as already found in other similar prototypical materials like Bi_2Se_3 [30], $Bi_2Te_2Se_2$ [31], and even for the n-type Bi_2Te_3 [27]. This proves that the long-lived SS population is a general property of the Bi_2Te_3 compound regardless its chemical doping level (n-type or p-type), and may be a universal feature of TIs.

Next, we compare the temporal evolution of the excess electronic population in two isoenergy regions at 28 meV above E_F marked as SS_2 and CB_2 [Table I], which

TABLE I: Characteristic decay times of SS_1, CB_1, SS_2 and CB_2 of the series of Bi_2Te_3 specimens. For each BT sample, the τ_1 (the ultrafast regime) and τ_2 (the long lasting regime) correspond to the values of the lifetimes of the first and the second raw, respectively.

Sample	τ_{SS_1} (ps)	τ_{CB_1} (ps)	τ_{SS_2} (ps)	τ_{CB_2} (ps)
BT0	2.08 ± 0.06	1.91 ± 0.05	6.78 ± 0.23	3.66 ± 0.29
	29.74 ± 10.4		45.16 ± 3.69	22.85 ± 3.45
BT1	2.03 ± 0.06	1.7 ± 0.04	7.88 ± 0.3	3.98 ± 0.1
BT2	2.65 ± 0.07	2.21 ± 0.05	2.45 ± 1.57	2.93 ± 0.26
			12.48 ± 0.61	12.97 ± 1.34

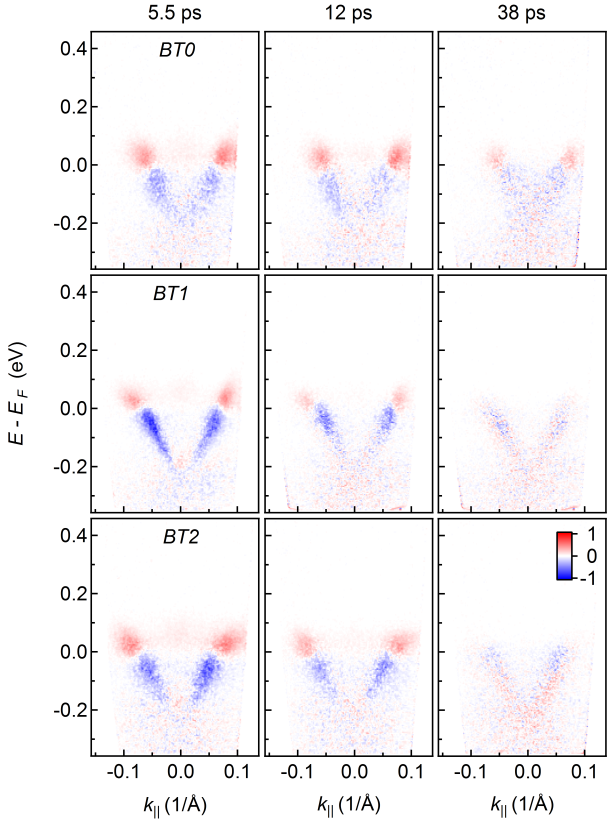

FIG. 3: (color online). Comparison of the ultrafast trARPES images, at three selected pump-probe time delays, for the non-irradiated and the irradiated Bi_2Te_3 series. Excess electrons (red) and holes (blue) are obtained from the difference of trARPES images taken after and before excitation.

present a qualitatively similar behavior between them for all samples. This indicates a very strong and effective interband scattering between SS_2 and CB_2. In particular, for the ultrafast temporal decay dynamics τ_1, the relaxation lifetimes for CB_2 for the three specimens are more or less identical (∼3 ps). In addition, the long decay rates τ_2 significantly differ from one sample to another: in particular, moving from the BT0 to the BT1, we can notably detect that τ_2 decreases for BT2 and completely vanishes for BT1. A parallel behavior for τ_1 and τ_2 can be also observed for SS_2, with different numerical values for τ_1 (∼ 7 ps) and τ_2 (45.16 ps and 12.48 ps).

Effectively, from the temporal decay behaviors [Table I], we can conclude that there are two regimes: the "ultrafast regime" τ_1 where BT1 and BT2 behave like BT0, and the "long lasting regime" τ_2 which is very sensitive to the irradiation conditions of the specimen.

Further insight into these two regimes can be obtained from the differences of the trARPES images with respect to negative delays, presented in Fig. 3. Blue and red areas correspond to a depleted and excess electronic populations, respectively, upon photoexcitation. At 5.5 ps, corresponding to the ultrafast regime, the three specimens show undifferentiated excess electronic population in the Dirac cone. For longer delays, precisely at 12 ps, we observe that the concentration of the Dirac fermions in BT0 and BT2 samples is higher than the one of the BT1 specimen. Moving to the extremely extended delays of the overlong regime, BT0 displays a persistent hot electron density in the Dirac SSs and a transient charge asymmetry—attributed to a spatial separation between excess electrons and holes. Irradiated samples, on the other hand, are been relaxed back to equilibrium.

Overall, this provides the very interesting information that the ultrafast relaxation of Dirac fermions in the SSs of Bi_2Te_3 is very sensitive to the irradiation conditions of bulk of the specimen. While the very long τ_2 of SS_2 is a property that has already been observed and can be explained by the fact that in the non-irradiated BT0 sample there are less defects, the different τ_2 for the irradiated BT1 and BT2 samples means that this parameters depends on the nature of the defects created by irradiation. Even though not all the aspects related to the long-term evolution of irradiation induced defects are clear, it was suggested that the vacancy insterstitial (Frenkel) pairs produced in the BT1 samples slowly evolve with time towards a majority of di-vacancies. It is consequently natural to associate the fastest relaxation time to the action of the former, while the latter makes it possible to mantain an intermediate regime for the SS_2 dynamics. Conversely, this also indicates that, by modifying the irradiation parameters (projectile dose, quantity of Frenkel pair-production, dwelling time at room temper-

ature, etc.), we can control the decay dynamics of the topological SSs.

IV. CONCLUSION

In summary, by means of an experimental trARPES study, we have investigated in detail the time-dependent electronic distribution after photoexcitation of a series of Bi_2Te_3 samples in different conditions of electronic irradiation. Our results confirm that the topological nature of the SSs is robust against the exposure to high-energy particles. Two dominating relaxation regimes govern the temporal evolution of the electron population of the series: the faster one is common for the three samples, i.e., unaffected by defect generation, and mainly determined by the characteristic time of the electron-phonon interaction; the slower one is related to the thermalization of the excess charge via diffusion and can be suppressed by adding disorder to the lattice. We conclude that we can modulate the electronic dynamics, in particular those of the topological SSs, by modifying the irradiation parameters. As all these parameters can be adjusted in a controlled way, they can potentially be used as a powerful tool in future devices based on photoconductive control of topological surface states with ultrafast light pulses.

Acknowledgments. We acknowledge financial support by the RTRA Triangle de la Physique, the EU/FP7 under the contract Go Fast (Grant No. 280555), by "Investissement d'Avenir" Labex PALM (ANR-10-LABX-0039-PALM), by the Equipex ATTOLAB (ANR11-EQPX0005-ATTOLAB) and by the ANR Iridoti (Grant ANR-13-IS04-0001).

[1] J. E. Moore, Nat. Phys. **5**, 378 (2009).
[2] M. Z. Hasan and C. L. Kane, Rev. Mod. Phys. **82**, 3045 (2010).
[3] J. E. Moore, Nature (London) **464**, 194 (2010).
[4] X.-L. Qi and S.-C. Zhang, Rev. Mod. Phys. **83**, 1057 (2011).
[5] M. Fruchart and D. Carpentier, C. R. Phys. **14**, 779 (2013).
[6] A. Bansil, H. Lin, and T. Das, Rev. Mod. Phys. **88**, 021004 (2016).
[7] D. Hsieh, Y. Xia, D. Qian, L. Wray, J. H. Dil, F. Meier, J. Osterwalder, L. Patthey, J. G. Checkelsky, N. P. Ong, A. V. Fedorov, H. Lin, A. Bansil, D. Grauer, Y. S. Hor, R. J. Cava, and M. Z. Hasan, Nature (London) **460**, 1101 (2009).
[8] P. Roushan, J. Seo, C. V. Parker, Y. S. Hor, D. Hsieh, D. Qian, A. Richardella, M. Z. Hasan, R. J. Cava, and A. Yazdani, Nature (London) **460**, 1106 (2009).
[9] J. Seo, P. Roushan, H. Beidenkopf, Y. S. Hor, R. J. Cava, and A. Yazdani, Nature (London) **466**, 343 (2010).
[10] H. Zhang, C.-X. Liu, X.-L. Qi, X. Dai, Z. Fang, and S.-C. Zhang, Nat. Phys. **5**, 438 (2009).
[11] D. O. Scanlon, P. D. C. King, R. P. Singh, A. de la Torre, S. McKeown Walker, G. Balakrishnan, F. Baumberger, and C. R. A. Catlow, Adv. Mater. **24**, 2154 (2012).
[12] J. G. Analytis, R. D. McDonald, S. C. Riggs, J.-H. Chu, G. S. Boebinger, and I. R. Fisher, Nat. Phys. **6**, 960 (2010).
[13] N. P. Butch, K. Kirshenbaum, P. Syers, A. B. Sushkov, G. S. Jenkins, H. D. Drew, and J. Paglione, Phys. Rev. B **81**, 241301(R) (2010).
[14] M. Caputo, M. Panighel, S. Lisi, L. Khalil, G. Di Santo, E. Papalazarou, A. Hruban, M. Konczykowski, L. Krusin-Elbaum, Z. S. Aliev, M. B. Babanly, M. M. Otrokov, A. Politano, E. V. Chulkov, Andrés Arnau, V. Marinova, P. K. Das, J. Fujii, I. Vobornik, L. Perfetti, A. Mugarza, A. Goldoni, and M. Marsi, Nano. Lett. **16**, 3409 (2016).
[15] Y. L. Chen, J. G. Analytis, J.-H. Chu, Z. K. Liu, S.-K. Mo, X. L. Qi, H. J. Zhang, D. H. Lu, X. Dai, Z. Fang, S. C. Zhang, I. R. Fisher, Z. Hussain, Z.-X. Shen, Science **325**, 178 (2009).
[16] J. G. Checkelsky, Y. S. Hor, M.-H. Liu, D.-X. Qu, R. J. Cava, and N. P. Ong, Phys. Rev. Lett. **103**, 246601 (2009).
[17] D. Kong, J. C. Randel, H. Peng, J. J. Cha, S. Meister, K. Lai, Y. Chen, Z.-X. Shen, H. C. Manoharan, and Y. Cui, Nano. Lett. **10**, 329 (2010).
[18] D. Kim, S. Cho, N. P. Butch, P. Syers, K. Kirshenbaum, S. Adam, J. Paglione, and M. S. Fuhrer, Nat. Phys. **8**, 459 (2012).
[19] Z. Chen, L. Zhao, K. Park, T. A. Garcia, M. C. Tamargo, and L. Krusin-Elbaum, Nano. Lett. **15**, 6365 (2015).
[20] L. Khalil, E. Papalazarou, M. Caputo, N. Nilforoushan, L. Perfetti, A. Taleb-Ibrahimi, V. Kandyba, A. Barinov, Q. D. Gibson, R. J. Cava, and M. Marsi, Phys. Rev. B **95**, 085118 (2017).
[21] L. Zhao, M. Konczykowski, H. Deng, I. Korzhovska, M. Begliarbekov, Z. Chen, E. Papalazarou, M. Marsi, L. Perfetti, A. Hruban, A. Wołoś, and L. Krusin-Elbaum, Nat. Commun. **7**, 10957 (2016).
[22] R. Haight, Surf. Sci. Rep. **21**, 275 (1995).
[23] J. A. Sobota, S. Yang, J. G. Analytis, Y. L. Chen, I. R. Fisher, P. S. Kirchmann, and Z.-X. Shen, Phys. Rev. Lett. **108**, 117403 (2012).
[24] J. Faure, J. Mauchain, E. Papalazarou, W. Yan, J. Pinon, M. Marsi, and L. Perfetti, Rev. Sci. Instrum. **83**, 043109 (2012).
[25] E. Papalazarou, J. Faure, J. Mauchain, M. Marsi, A. Taleb-Ibrahimi, I. Reshetnyak, A. van Roekeghem, I. Timrov, N. Vast, B. Arnaud, and L. Perfetti, Phys. Rev. Lett. **108**, 256808 (2012).
[26] M. Marsi, L. Nahon, M.E. Couprie, D. Garzella, T. Hara, R. Bakker, M. Billardon, A. Delboulbé, G. Indlekofer, and A. Taleb-Ibrahimi, J. Electron. Spectrosc. Relat. Phenom. **94**, 149 (1998).
[27] M. Hajlaoui, E. Papalazarou, J. Mauchain, G. Lantz, N. Moisan, D. Boschetto, Z. Jiang, I. Miotkowski, Y. P. Chen, A. Taleb- Ibrahimi, L. Perfetti, and M. Marsi, Nano Lett. 12, 3532 (2012).
[28] A. Crepaldi, B. Ressel, F. Cilento, M. Zacchigna, C. Grazioli, H. Berger, Ph. Bugnon, K. Kern, M. Grioni, and F. Parmigiani, Phys. Rev. B **86**, 205133 (2012).
[29] M. Hajlaoui, E. Papalazarou, J. Mauchain, L. Perfetti, A. Taleb-Ibrahimi, F. Navarin, M. Monteverde, P. Auban-Senzier, C. R. Pasquier, N. Moisan et al., Nat. Commun.

5, 3003 (2014).
[30] J. A. Sobota, S.-L. Yang, D. Leuenbergera, A. F. Kemperd, J. G. Analytise, I. R. Fisher, P. S. Kirchmanna, T. P. Devereauxa, and Z.-X. Shen, J. Electron. Spectrosc. Relat. Phenom. **195**, 249 (2014).
[31] M. Neupane, S.-Y. Xu, Y. Ishida, S. Jia, B. M. Fregoso, C. Liu, I. Belopolski, G. Bian, N. Alidoust, T. Durakiewicz, V. Galitski, S. Shin, R. J. Cava, and M. Z. Hasan, Phys. Rev. Lett. **115**, 116801 (2015).